SNOW SURFACE TEMPERATURE FROM AVHRR AS A PROXY FOR SNOWMELT IN THE ALPS

D. Oesch, S. Wunderle, A. Hauser

Remote Sensing Research Group, Departement of Geography, University of Berne, Hallerstrasse 12, 3012 Berne, Switzerland, phone: ++41-31-631-80-20, fax: ++41-31-631-8511, e-mail: oesch@giub.unibe.ch

ABSTRACT

Infrared radiance measurements from satellites can be used for estimation of snow surface temperatures, a proxy for snow melting. NOAA - AVHRR data was processed using Split – Window – Technique (SWT) for reducing atmospheric attenuation and generating snow surface temperatures. Up to now, the retrieval of snow surface temperatures using the SWT on AVHRR data has only be done for polar regions. These temperatures cannot only be used for calibrating and calculating snow surface energy budget models, it is also possible to monitor the snow melting process itself. The temporal and spatial distribution, respectively of the snow surface temperatures can be used as a proxy for a beginning ablation period.

In this study, we used NOAA-AVHRR noon data covering an area in the center of the Alps. The extent of snow cover has been derived by a simple threshold method based on emissivities derived from the visible channels. No additional data, such as in situ data, was used.

Results obtained with the described method show the spatial and temporal variability of the snow surface temperature within the Alpine region. Areas with potential snowmelt have been identified, analysed concerning their validity and the use of a subpixel analysis is finally suggested. Other data, such as information from meteorological stations or numerical model output in combination with snow surface temperatures can be helpful to forecast the development of the runoff related to a major river catchment.

INTRODUCTION

Water stored in snow cover is an important contributor to runoff in an alpine basin. Thus decision makers concerned with flood managing or hydropower companies show strong interest in this process. During the flood events during spring of 1999 in the watershed of the river located in the Alps, snowmelt proved to be an important factor for the discharge. The area of interest of this paper will therefore be the catchment basin of the Aare, as shown in Figure 1.
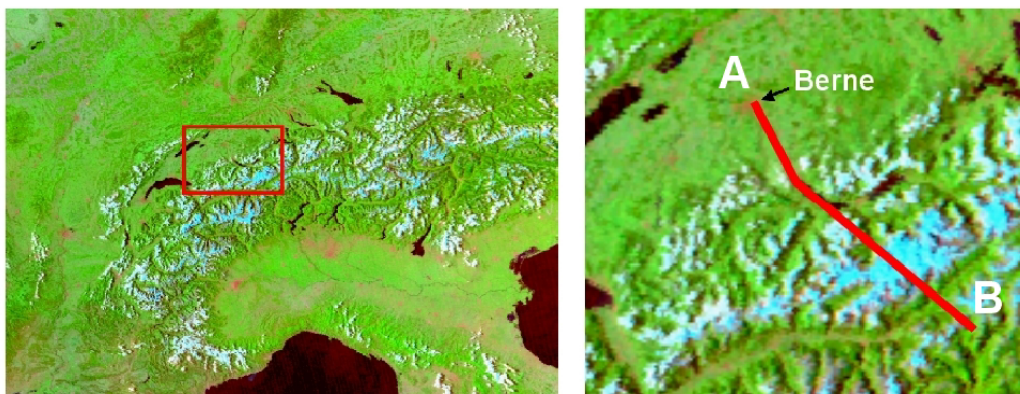
Figure 1:   The situation of the area of interest (AOI) (right) located in the Alps (left) (NOAA-12, July 30th 2001, 15:52 UTC, R: ref3, G:ch2, B: ch1).

The snowmelt process is the trigger for a contribution of snow cover to runoff. In order to establish reliable flood predictions, information on this parameter is very useful. The melting process of the surface can be easily observed in the longwave portion of the spectrum, since snow is almost an ideal blackbody. In this case, snow surface temperature is set at 0°C (273.2K) and if it is assumed that emissivity (ε) = 1, the value of the longwave outgoing radiation is constant at 316Wm^2. The occurrence of the temperature maximum of the subsurface temperature profile of a deep snow pack is just beneath the surface. This feature is a result of the fact that by day radiative heat transfer dominates over heat conduction in the upper 0.5m of snow, and also because short-wave radiation is transmitted much more readily than long-wave radiation in this media. The strong absorption of snow in the infrared only allows radiative loss to occur from a thin surface layer. One consequence is that a snow cover with a melting surface does not necessarily melt over the whole snow pack. This is only the case, if the snow layer is considerably thin. Secondly, an observed snow cover melting during a daytime satellite pass can refreeze overnight.

The purpose of this paper is to prove the feasibility of the NOAA-AVHRR sensor for monitoring snowmelt processes. Up to now, observing snow cover temperature using the AVHRR sensor was done mainly in polar regions (1), (2), (3), and (4). No research results are done for midlatitudes mountain regions. Calculating the snow surface temperatures from the two thermal channels, the status of snow cover in a certain basin can be determined. No additional data, such as in situ measurements or parameters from models will be used.

Ever since thermal infrared data have been available, several approaches have been developed to infer surface temperature. The first problem to be solved is to translate the satellite radiance into surface brightness temperature. For this after calibration and conversion of radiance into temperature using inverse Planck's law, it is necessary to account for atmospheric contribution. Then it is necessary to transform surface brightness temperature into surface temperature and thus to take into account emissivity and directional effects. Actually, the problem is slightly more complicated, as atmospheric, emissivity, and directional effects are coupled and these perturbing factors cannot be tackled independently.

METHODS

In the present study NOAA – 14 data was used, unless mentioned otherwise. The data has been calibrated according to (5). A BRDF (6) correction and SMAC (7) have been performed and the C-factor method was used for the terrain normalization. Finally, an orthorectification of the data is essential in an alpine region. The cloud mask was generated using CASPR (cloud and surface parameter retrieval routine) (8). Atmospheric influence on the thermal channels are corrected using a Split - Window - Technique (SWT) algorithm. The SWT relies on the different absorption characteristics of the atmosphere within two different but close wavelengths. The algorithm consists simply of a linear combination of the thermal channels, which gives a surface temperature pseudo corrected for atmospheric contribution. For the AVHRR/2 the equation according to (9) is of the type:

$$T_{Surface} = 1.274 + \left[\frac{T_{Ch4} + T_{Ch5}}{2}\left(1 + 0.015616\left(\frac{1-\varepsilon}{\varepsilon}\right) - 0.482\left(\frac{\Delta\varepsilon}{\varepsilon^2}\right)\right) + \frac{T_{Ch4} - T_{Ch5}}{2}\left(6.26 + 3.98\left(\frac{1-\varepsilon}{\varepsilon}\right) + 38.33\left(\frac{\Delta\varepsilon}{\varepsilon^2}\right)\right)\right] \quad (1)$$

$$\Delta\varepsilon = \varepsilon_{Ch4} - \varepsilon_{Ch5}, \varepsilon = \frac{\varepsilon_{Ch4} + \varepsilon_{Ch5}}{2}$$

where T_{Ch4} and T_{Ch5} are the brightness temperatures at the top of the atmosphere in the two infrared bands. This SWT algorithm is dependent on emissivity of the different channels (ε_{Ch4} and ε_{Ch5}). The emissivity itself is dependent on snow properties and viewing angle, whereas angular effects may dominate at the wavelengths of the AVHRR (10), (11) and (12). Snow surface emissivity values have been variously given in the range 0.97 to 1, with 0.99 being the most frequently quoted (13). In this study, an emissivity of 0.99 has been assigned to the snow cover, but it has to be considered

that a melting snow surface can possess an emissivity as low as 0.95. The snow cover itself was de-rived using a simple threshold method: If emissivities are calculated using the visible channels ac-cording to (14), all non-vegetation and non–soil pixels such as waterbodies and snow surfaces can clearly been discriminated.

Using data from the winter 1999, the two following case studies will be discussed.

Snow Cover Temperature February 12 and 15, 1999

On 09.02.99, heavy snow fall even in the lower parts of the central Alps occurred. The snow surface temperatures three days later on 12.02.99 for the AOI in Figure 1 are shown on top left of Figure 2: Dark areas represent pixels covered with clouds or pixel with temperatures warmer than 0°C. The 500m contour lines (red) are superimposed. Temperatures in the lower regions are around –10°C, in higher altitudes around –20°C. Differences related to topography such as altitude and aspect can be recognized. Three days later, dominated by strong solar irradiance, the snow surface temperature situation for this area changed drastically as can be seen on top right of Figure 2: Temperatures in the lower areas have an average of –3°C and are close to 0°C in some regions: It can be assumed that the snow surface melted at these locations. Especially around the city of Berne (A), snow cover had gone during those three days. In the higher located parts, snow surface temperature dropped by nearly 10°C.

The white lines in the top maps of Figure 2 represent the bottom transects. The altitude of the tran-sect ranging from Berne over the Jungfrau region to the valley of Wallis in the south is plotted in dotted lines. Snow surfaces temperatures are shown in red. An increase in temperatures during this three-day period can be observed, especially in the lower regions. Pixels along the transect with melting snow skin surfaces as well the temperature correlation with the topography can be identi-fied.

The existence of snow cover pixels with temperatures higher than 0°C is due to the limitations of the spatial resolution of the AVHRR. Non–snow surfaces within a mixed pixel distort the snow sig-nal.
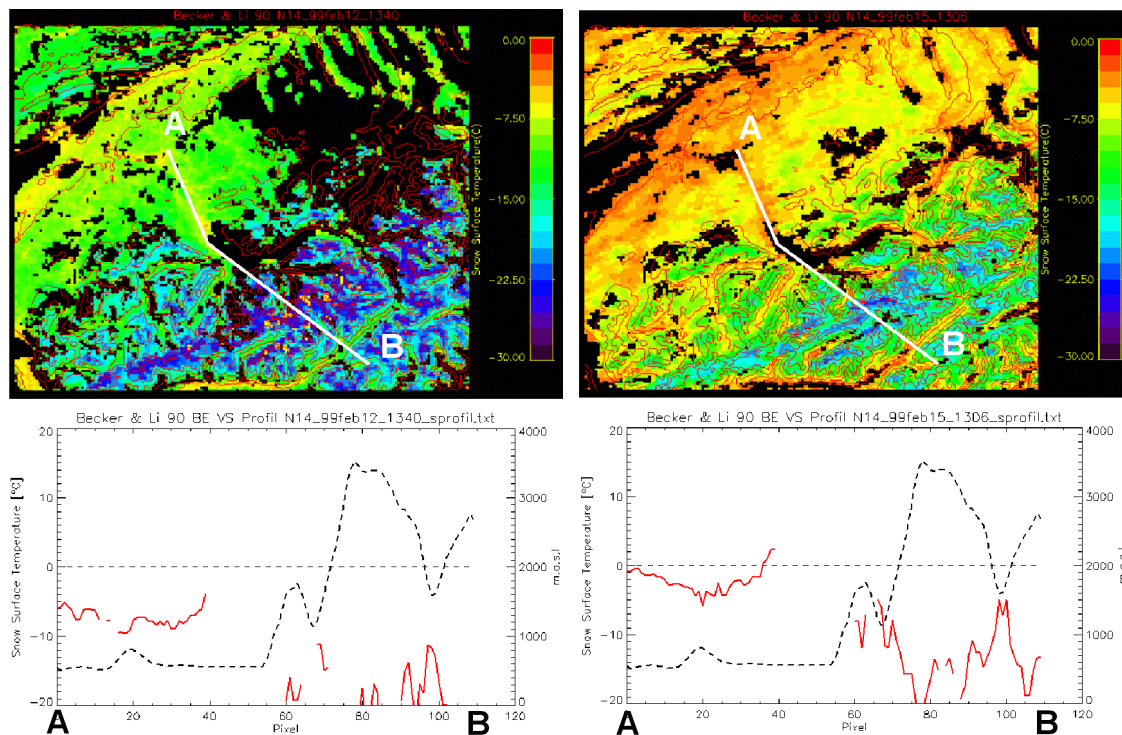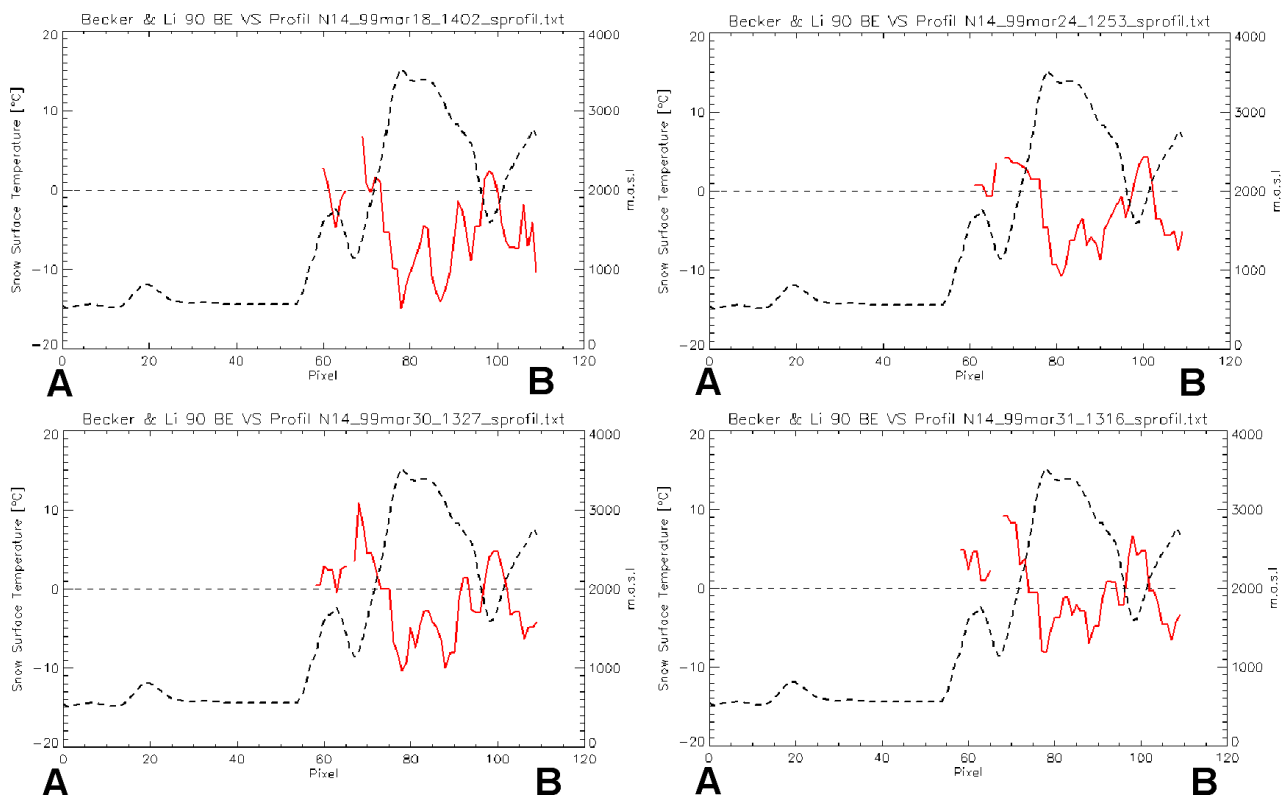

Figure 2: *Snow surface temperature for the AOI in Figure 1 on 12.02.99 on 13:40 UTC (*top left*) and on 15.02.99 13:06 UTC (*top right*) with corresponding profiles (*bottom left *and* right*).*

Snow Cover Temperature Mach 18 - 31 1999

At the end of March 1999 warm weather was predominating in combination with clear sky condition on 18th, 24th, 30th and 31st of March. Concerning the general development of the snow cover temperature for the transect in Figure 1, a general increase of temperature independent of the altitude during these 13 days can be recognized (Figure 3). On all four satellite passes, a warmer peak within the Jungfrau region due to the local southward orientation of the surface is the case. It follows that surface temperatures on the valley in the south (right) differ from the surrounding pixels: The higher longwave emittance of patches of non-snow surfaces is responsible for the stronger heating.

A crude calculation to determine the variation of the melting border altitude can be done the following way: When a perpendicular is drawn from the intersection between the temperature curve with the straight 0°C temperature line, a new intersection with the dotted topography curve indicates the theoretical altitude. Considering this, the melting border of the valley located in the south increases by around 100m from 1,900 m a.s.l. to 2,000 m a.s.l., first on the south rim and from the 24th on also on the north rim.

On the north slope of the Jungfrau region, the same effect can be identified. The temperature line in the valley nearby is interrupted due to the fact that no snow was detected using the threshold method in the visible channels. It can be assumed that on the mountain located south of this depression only pixels with patches of snow exist and therefore temperatures are again above 0°C.

Figure 3:   Snow surface temperatures for the transect in Figure 1 for 18.03.99 14:02 UTC (top left), 24.03.99 15:53 UTC (top right), 30.03.99 13:27 UTC (bottom left) and 31.03.99 13:16 UTC (bottom right).

Mixed Pixel Problem

One of the main problems using the AVHRR sensor is its medium spatial resolution (1.1 × 1.1km) in a region with heterogeneous topography and surface. Only pure snow pixels, which are melting, will have temperatures around 0°C, but due to the alpine topography, such pixels are not the normal case. In addition, snow surfaces within a pixel contain dark patches made of bare soil, rock or trees.

Those areas, in contrast to the snow cover, absorb the solar irradiation and therefore emit high amounts of longwave radiation.

For this reason, a pixel assigned as a snow pixel using a threshold method based on the visible channels, feature temperatures above 0°C according to the thermal channels. This fact can be observed for the AOI in Figure 1 on 26.06.01 as shown in

Figure 4. A subpixel classification of snow according to (15), (16), and (17) clearly shows the strong relationship between the amount of snow within a pixel and its temperature. Temperature decreases with increasing snow cover within a pixel. Only a few pixels are fully snow covered and show temperatures around 0°C. Considering the 2m air temperature of the meteorological station on the Jungfraujoch (3,580 m a.s.l.) for this day (Figure)???, it can be assumed that a pure snow pixel will undergo snow melting and therefore have temperatures around 0°C. The maximum air temperature occurred approximately at the same time as one of the satellite passes in the afternoon. The preceding days were also dominated by strong solar irradiation and warm air temperature, indicated by the air temperature of the Jungfraujoch which never went below 0°C during 24 hours. The high temperatures of the pixels covered only partly with snow are due to the dark areas within these pixels as mentioned above.

A comparison of the temperature variation during this day (26.06.01) between a mixed pixel and a pure snow pixel can be seen in   Figure . During this day, snow surface temperatures for the AOI from five satellite passes were calculated: 02:32 UTC (N-16), 04:18 UTC (N-14), 12:22 UTC (N-16), 15:42 UTC (N-12), and 16:48 UTC (N-14). Using the subpixel classification algorithm, a pure snow pixel and a mixed snow pixel (70%) in the Bernese Alps were identified. Both pixels are located at an altitude of around 2,500 m a.s.l. On this day, both the mixed and the pure pixel feature nearly the same surface temperature on morning and noon satellite passes. But there are significant differences in the late afternoon. The pure snow pixel has a temperature below but close to 0°C, while the mixed pixel is way above 0°C. Here again, the heating of the different surfaces such as snow and soil / bare rock can be assumed to vary as explained above.
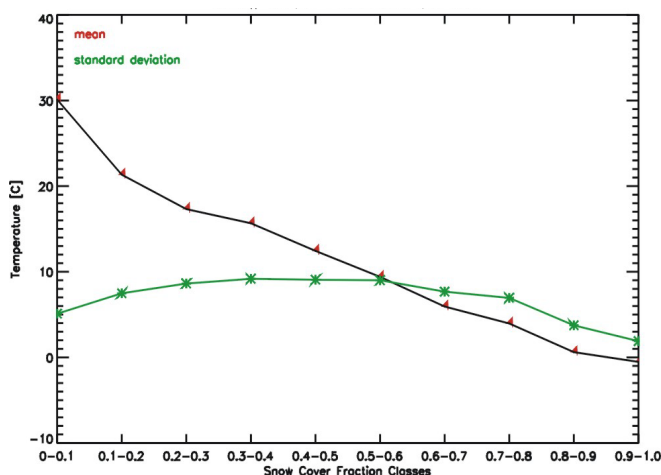

Figure 4: *Snow cover fraction Classes for the AOI on 26.06.01, 1542 UTC derived from NOAA – 12.*
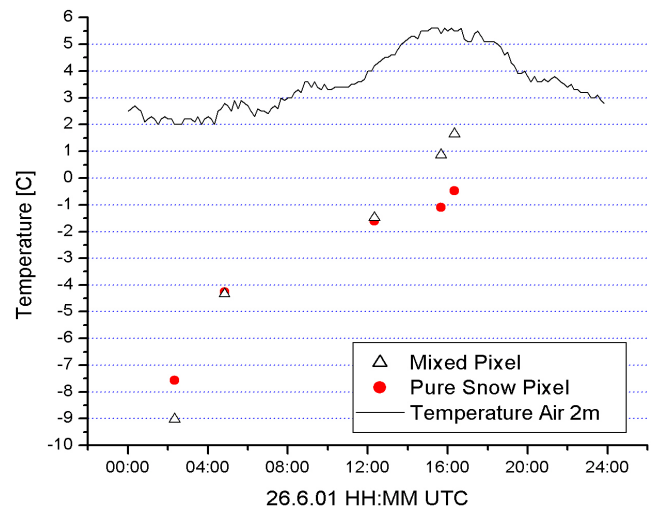
Figure 5: *Daily variation of snow surface temperature for a mixed and a pure snow pixel in comparison to 2m air temperature on 26.06.21.*

CONCLUSIONS

Due to the limitations of spatial resolution of the AVHRR – sensor, the following conclusions can be drawn: Using the NOAA – AVHRR sensor for monitoring snowmelt is only valid for pure snow pixels in the alpine region, if no separation of the different thermal contributions within a pixel is

made. The signal contributed from surfaces other than snow within a pixel distorts the snow signal significantly. Therefore, a subpixel estimation of the snow cover is essential. Only in the case of a pure snow pixel is the origin of the longwave radiation contribution clear. With this method, an operational estimation of snow cover temperature is possible.

The properties of the snow cover concerning its status of melting cannot be monitored, if the different surfaces within a pixel are not taken into account.

Another consideration is related to the nature of the structure of snow cover: A melting skin snow surface does not necessarily contribute to the discharge of the local basin. No reliable information for the whole snow pack can be retrieved from the AVHRR alone.

Other data such as information from meteorological stations or numerical models in combination with snow surface temperatures can be helpful to forecast the development of the runoff in a major river catchment.

ACKNOWLEDGEMENTS

REFERENCES

1. Stroeve, J. and Steffen K. 1998. Variability of AVHRR-derived clear sky surface temperature over the Greenland ice sheet. Journal of Applied Meteorology. 37(1):23-31.

2. Haefliger, M., Steffen K. and Fowler C. 1993. AVHRR surface temperature and narrow-band albedo comparison with ground measurements for the Greenland ice sheet. Annals of Glaciology. 17:49-54.

3. Key, J.R. and Collins J.B. 1997. High-latitude surface temperature estimates from thermal satellite data. Remote Sensing of Environment. 61:302-309.

4. Key, J. and Haefliger M. 1992. Arctic ice surface temperature retrieval from AVHRR thermal channels. Journal of Geophysical Research. 97(D5):5885-5893.

5. ESA EPO. SHARP Level-2 User Guide, Release 1.0, 1992.

6. Wu, A., Li Z. and Cihlar J. 1995. Effects of land cover type and greenness on advanced very high resolution radiometer bidirectional reflectances: analysis and removal. Journal of Geophysical Research. 100(5D):9179-9192.

7. Rahman, H. and Dedieu G. 1994. SMAC: a simplified method for the atmospheric correction of satellite measurements in the solar spectrum. International Journal of Remote Sensing. 15(1):123-143.

8. Key, J.R. The cloud and surface parameter retrieval (CASPR) system for polar AVHRR - User's Guide, NOAA/NESDIS/ORA/ARAD/ASPT, 2001.

9. Becker, F. and Li Z.-L.. 1990. Towards a local split window method over land surfaces. International Journal of Remote Sensing. 11(3):369-393.

10. Dozier, J. and Warren S.G. 1982. Effect of viewing angle on the infrared brightness temperature of snow. Water Resources Research. 18(5):1424-1434.

11. Wald, A. 1994. Modeling thermal infrared (2-14 mm) reflectance spectra of frost and snow. Journal of Geophysical Research. 99:24241-24250.

12. Salisbury, J.W. and D'Aria M.D. 1992. Emissivity of terrestrial materials in the 8 - 14 μm atmospheric window. Remote Sensing of Environment. 42:83-106.

13. Collier, P., Runacres A.M. and McClatchey J. 1989. Mapping very low surface temperature in the Scottish Highlands using NOAA AVHRR data. International Journal of Remote Sensing. 10(9):1519-1529.

14. Valor, E. and Caselles V. 1996. Mapping land surface emissivity from NDVI: Application to European, African, and South American areas. Remote Sensing of Environment. 57(3):167-184.

15. Adams, J., B. and Smith M. O. 1986. Spectral mixture modeling: A new analysis of rock and soil types at the Viking Lander 1 site. Journal of Geophysical Research. 91(B8):8098-8112.

16. Settle, J., and Drake N. 1993. Linear mixing and estimation of ground cover proportions. International Journal of Remote Sensing. 14(6):1159-1177.

17. Gong, P. et al. 1991. Spectral Decomposition of Landsat Thematic Mapper data for urban land-cover mapping. Proceedings of the 14th Canadian Symposium on Remote Sensing: 458-461. Calgary, Alberta, Canada.